Check for updates

Influence of the secondary ligand, phenanthroline, on the antioxidant and pro-oxidant and cytotoxic effects of the oxidovanadium(IV)/naringin complex†

Andrés G. Restrepo, [a] Angel L. Huamani, [a] Alexandra Velásquez Bravo, [a]
Pablo J. González, [b] Luciana G. Naso, *[a] Evelina G. Ferrer [a] and
Patricia A. M. Williams *[a]

The complex [VONargPhenCl] (Narg, naringin; phen = 1,10-phenanthroline) was synthesized and characterized. Comparative analysis with the binary complex, [VO(Narg)$_2$], revealed improvements in both antioxidant and anticancer effects upon replacing one Narg ligand with Phen. The new complex behaved as a better antioxidant against reactive oxygen species (ROS) and displayed higher cytotoxicity (against the A549 human lung cancer cell line, 24 h incubation) compared to the ligands and the binary complex. This increased cytotoxic effect was associated with intracellular ROS generation and GSH/GSSG depletion, indicating an oxidative stress mechanism. Additional observations, such as the depletion of mitochondrial membrane potential and morphological changes, suggested the involvement of an intrinsic apoptotic pathway. Furthermore, the complex exhibited enhanced cellular uptake of vanadium compared to the binary complex. The complex demonstrated spontaneous interaction with bovine serum albumin and the binding constant values indicated its ability to be transported by this protein. This study underscores the significance of incorporating a compound with π-electronic delocalization into the coordination sphere of the oxidovanadium(IV) cation that improves the antioxidant capacity. Moreover, its lipophilic characteristics impart an improved transport across the cellular membrane and enhance the pro-oxidant effects in cancer cells, ultimately enhancing the anticancer actions of the metal complex.

[a] *Centro de Química Inorgánica (CEQUINOR, UNLP, CONICET, asociado a CICPBA), Departamento de Química, Facultad de Ciencias Exactas, Universidad Nacional de La Plata, Bv. 120 No 1465, CP 1900 La Plata, Buenos Aires, Argentina. E-mail: williams@quimica.unlp.edu.ar, lucianabaso504@hotmail.com*

[b] *Departamento de Física, Facultad de Bioquímica y Ciencias Biológicas, Universidad Nacional del Litoral and CONICET, S3000ZAA Santa Fe, Argentina*

† Electronic supplementary information (ESI) available: Experimental section. Fig. S1 (ESI). Thermogravimetric analysis (TGA) curve for the thermal decomposition of [VONargPhenCl]·3H$_2$O. Oxygen flow: 50 mL min^{-1}, rate: 10 °C min^{-1}. Fig. S2 (ESI). Infrared spectra of naringin, [VO(Narg)$_2$]·8H$_2$O, 1,10-phenanthroline and the ternary complex [VONargPhenCl]·3H$_2$O. Fig. S3 (ESI). Electronic spectra of the VONargPhenCl complex in (2.5 × 10^{-3} M, DMSO) and (2.5 × 10^{-3} M, 1% DMSO–99% H$_2$O) for 2 h, 25 °C. Fig. S4 (ESI). Effects of VONargPhenCl on DPPH$^{\bullet}$, the reduction in the concentration of the DPPH$^{\bullet}$ radical (517 nm); $^{\bullet}$OH, the development of a pink chromogen (λ = 532 nm) from the reaction of deoxyribose, hydroxyl radicals and thiobarbituric acid (TBA); O$_2^{\bullet -}$, the reduction of nitroblue tetrazolium by the generated superoxide radical at 560 nm; ROO$^{\bullet}$, AAPH-generated peroxyl radical-pyranine mixture. Time delay (lag pahse) of pyranine consumption, measured at 454 nm. The values are expressed as the mean ± SEM of at least three independent experiments. Fig. S5 (ESI). Plots of log[($F_0 - F$)/F] *vs.* log(Q) for the interaction of BSA with VONargPhenCl at different temperatures, λ_{ex} = 280 nm. See DOI: https://doi.org/10.1039/d4nj00655k

Introduction

Naringin, a flavonoid compound abundantly found in citrus fruits, especially grapefruit, is a glycoside composed of a flavonoid aglycone known as naringenin and a sugar molecule called rutinose. The presence of this glycosidic linkage endows naringin with its distinctive bitter taste. Upon interaction with gut flora, naringin undergoes hydrolysis to form naringenin. However, due to its large hydrophobic ring structure, naringin's bioavailability is limited, affecting its absorption and metabolism within the body.[1] Despite this, naringin has garnered attention for its potential health benefits, attributed to its diverse biological properties. These properties encompass antioxidant activity, anti-inflammatory effects, and promising anticancer potential.[2,3] Furthermore, naringin has shown promise in providing cardiovascular and neuroprotection.[4]

The binding of metal ions to bioactive compounds like naringin can introduce novel or enhanced biological functions to the ligands. Such coordination with biometals offers biological advantages, encompassing heightened functionality,
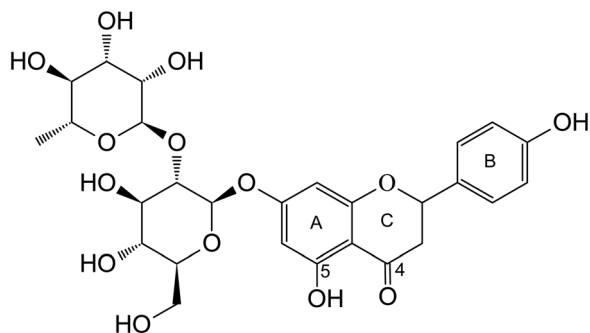
Fig. 1   Structure of naringin.

support of enzymatic activities, facilitation of electron transfer, structural stability, assistance in signal transduction, contribution to oxygen binding and transport, regulation of metal homeostasis, catalysis of reactions, participation in antioxidant defense, and influence on DNA processes within cells.[5] Phenanthroline is a bidentate ligand with the ability to form coordinated bonds with biometals. It can modify the electronic properties of a molecule acting as an electron-withdrawing ligand. Introducing phenanthroline as a second ligand can enhance the binding affinity of the biometal, stabilizing the coordination structure and enabling interaction with other molecules in the biological environment. This interaction can alter the complex's three-dimensional structure, potentially impacting its compatibility with active sites in proteins, DNA, or other macromolecules.[6]

In previous work, we successfully synthesized a metal complex involving naringin (Fig. 1) and the oxidovanadium(IV) cation, VONarg$_2$.[7] Our investigations revealed a substantial improvement in the anticancer effects of naringin through this complexation. Furthermore, we documented an enhancement in the flavonoid's antioxidant power against various radicals such as superoxide, peroxyl, and DPPH radicals. In assessing naringin's performance individually in the A549 lung cancer cell line, we noted limited anticancer activity within the tested concentrations.[8] However, the complex exhibited a reduction in cell viability, attributed to its pro-oxidant effects. In the context of our ongoing research, we have undertaken the synthesis and thorough characterization of a novel ternary complex, [VONargPhenCl]·3H$_2$O (VONargPhenCl). This new complex involves the substitution of one ligand Narg with the inclusion of phenanthroline (Phen). This modification could potentially lead to further enhancements in both the antioxidant and anticancer properties of VONarg$_2$. Our research endeavors encompassed investigations into mechanisms of action (ROS production, disruption of mitochondrial membrane potential, and cell redox state), cellular uptake and interactions with BSA, providing a comprehensive exploration of the complex's properties and potential applications.

Experimental section

Reagents

All chemicals employed in this study were of analytical grade. Oxidovanadium(IV) chloride (50% aqueous solution, Carlo Erba),

naringin (Sigma, St. Louis, MO, USA), and 1,10-phenanthroline monohydrate (Merck) were used as supplied. Elemental analysis for carbon, nitrogen and hydrogen was conducted using a Carlo Erba EA1108 analyzer. The methods for the general experiments are described in the ESI.† The vanadium content was quantified using the tungstophosphovanadic method (see the ESI† for the description of this method).[9] For thermogravimetric analysis, a Shimadzu system (model TG-50) operating at a heating rate of 10 °C min^{-1} within a 50 mL min^{-1} oxygen flow was used. Infrared spectra were acquired using the KBr pellet technique, employing a Bruker IFS 66 FTIR spectrophotometer, ranging from 4000 to 400 cm^{-1}. Fluorescence spectra were recorded using a Shimadzu RF-6000 spectrophotometer equipped with a pulsed xenon lamp. UV-Vis and diffuse reflectance spectra were recorded with a Shimadzu UV-2600/2700 spectrophotometer, using BaSO4 as the standard. The molar conductance of the complex was measured with a Conductivity TDS Probe – 850084, Sper Scientific Direct, using 1×10^{-3} M solutions of DMSO and H$_2$O–DMSO (99–1%). Microplate measurements were conducted using a Microplate reader Ivdiagnostik M201. For the X-band CW-EPR spectra, both powdered samples and DMSO or DMSO/H$_2$O solutions were examined at temperatures of 100 K and room temperature (ca. 298 K) on a Bruker EMX-Plus spectrometer. The spectrometer was equipped with a rectangular cavity featuring 100 kHz field modulation, and with standard Oxford Instruments low-temperature devices (ESR900/ITC4). The spectra were baseline corrected using WinEPR Processing software (Bruker, Inc). Simulation of the powder sample was performed with WinEPR Simfonia, while the spectra of frozen solutions were simulated using the EasySpin 5.2.3. toolbox based on MATLAB. Cell culture materials were obtained from Corning or Falcon, with Dulbecco's modified Eagle's medium (DMEM) sourced from Merck, Tryple™ from Invitrogen (Argentina SRL) and fetal bovine serum (FBS) from Internegocios, Argentina. All other chemicals used were of analytical reagent grade and were utilized without further purification.

Synthesis of [VONargPhenCl]·3H$_2$O, (VONargPhenCl)

1,10-Phenanthroline monohydrate (0.5 mmol) was suspended in 2.4 mL of water and 0.5 mmol of VOCl$_2$ was added, allowing the solution to stir until homogeneity was achieved. Then, a solution containing 0.5 mmol of naringin and 0.25 mmol of triethylamine in 5.6 mL of ethanol was added. After 60 min of stirring at room temperature, the final pH was adjusted to 6 using triethylamine. The resulting product was precipitated with 60 mL of acetonitrile and the solid was filtered, washed with acetonitrile and dried at 60 °C. Elemental analysis calc. for C$_{39}$H$_{39}$O$_{15}$N$_2$VCl·3H$_2$O: C, 51.1; H, 4.9; N, 3.1; V, 5.6; found: C, 51.3; H, 5.0; N, 3.1; V, 5.7%. UV-Vis data for the 1:1:1 V(IV)O^{2+} to naringin to Phen ratio, λ_{max} (DMSO)/nm 769 (ε/dm^3 mol^{-1} cm^{-1} = 88.4). Thermal analysis (TGA) under an oxygen atmosphere with a flow rate of 50 mL min^{-1} and a heating rate of 10 °C min^{-1} revealed a first mass loss of 6.0% at 108 °C, corresponding to the loss of three water molecules (% calc. 5.9) as shown in Fig. S1 (ESI†). After various degradation steps, a final residue value of 9.8% was obtained, which corresponds to the formation of V$_2$O$_5$

(% calc, 9.9). The presence of V$_2$O$_5$ in the residue was confirmed by FTIR spectroscopy. The molar conductance of the complex measured in DMSO, Λ_m = 0 Ω^{-1} cm^2 mol^{-1}, indicates a non-electrolyte nature for the complex. Based on these results, the formula [VONargPhenCl]·3H$_2$O is proposed for the solid complex.

Antioxidant determination

The antioxidant activities of the complex were assessed through various assays, including the superoxide dismutase (SOD) mimetic assay, hydroxyl radical scavenging, inhibitory effects on peroxyl radical (as reactive oxygen species) and the 1,1-diphenyl-2-picrylhydrazyl radical (DPPH) assay. Reported protocols were followed for these determinations.[10] Briefly, the capability of the complex to scavenge hydroxyl radicals was evaluated by quantifying the degradation of deoxyribose caused by hydroxyl radicals generated within the ascorbate-Fe–H$_2$O$_2$ system. The degree of deoxyribose degradation was measured at 535 nm. To indirectly determine SOD activity, the nitroblue-tetrazolium (NBT) assay was employed. The complex's inhibitory effect on the reduction of NBT by the superoxide anion, generated through the phenazinemethosulfate (PMS) and reduced nicotinamide adenine dinucleotide (NADH) system, was measured.

For assessing inhibitory activity against peroxyl radicals, the delay introduced by the compounds in pyranine consumption (known as the lag phase) caused by peroxyl radicals was quantified. The DPPH radical scavenging activity was determined in the presence and absence of the complex, with the latter value set as the reference at 100%.

Each experiment was performed in triplicate and a minimum of three independent experiments were carried out for each assay.

Interaction with bovine serum albumin (BSA)

To investigate the interaction between bovine serum albumin (BSA) and the complex [VONargPhenCl]·3H$_2$O (VONargPhenCl), the following experimental procedure was employed: BSA was incubated for 1 h at a final concentration of 6 µM in Tris-HCl buffer (0.1 M, pH 7.4) along with the complex at varying concentrations ranging from 0 to 100 µM (specifically, 5, 10, 15, 20, 25, 50, 75, and 100 µM). The incubation was conducted in the presence of DMSO at a final concentration of 0.5% v/v. This process was carried out at three distinct temperatures: 25 °C, 30 °C, and 37 °C (equivalent to 298 K, 303 K, and 310 K, respectively). Following the incubation, emission spectra were recorded utilizing a Shimadzu RF-6000 spectrofluorometer within the wavelength range of 290 to 450 nm, with an excitation wavelength of 280 nm. To maintain consistency, the excitation and emission bandwidths were both set at 10 nm, while the scanning speed was 6000 nm minute^{-1}, using a resolution of 1 nm. For each sample and concentration, a minimum of 5 replicates were measured across at least 3 independent experiments.

To calculate the binding constants and thermodynamic parameters, the observed fluorescence intensity at 336 nm (referred to as F_{obs}) was adjusted to account for the influence of the complex on the fluorescence intensity; a phenomenon termed the "inner filter effect." This correction was achieved using the formula: $F_{corr} = F_{obs} \times \exp[(A_{ex} + A_{em})/2]$, where A_{ex} and A_{em} represent the absorbance values of the sample at the excitation wavelength (280 nm) and the emission wavelength (336 nm), respectively.[11,12]

Cell culture

In a humidified 37 °C incubator with a 5% CO$_2$ environment, the human lung cancer cell line A549 and the human normal amnion cell line WISH[13] were grown in Dulbecco's modified Eagle medium (DMEM) supplemented with 10% fetal bovine serum (FBS), penicillin (100 U mL^{-1}), and streptomycin (100 g mL^{-1}). When cells achieved 70–80% confluence, they were washed with phosphate-buffered saline (PBS) (11 mM KH$_2$PO4, 26 mM Na$_2$HPO4, 115 mM NaCl, pH 7.4) and sub-cultured with TrypLE™. Cells were cultivated on multi-well plates for the studies. When the cells reached 70% confluence, the monolayers were washed twice with DMEM before being treated with the compounds.

Cell viability assay (MTT assay)

The 3-[4,5-dimethylthiazol-2-yl]-2,5-diphenyltetrazolium bromide (MTT) method (Sigma-Aldrich, St. Louis, MO, USA) was used to assess cell viability. For the treatments, cells were seeded at a density of 1.5×10^4 per well in 96 well plates, cultured overnight, and then incubated with the ternary complex and 1,10-phen-antrhroline chloride in FBS free media. After 24 h of incubation at 37 °C, 100 µg of MTT per well was added and incubated in a CO$_2$ incubator for 2 h at 37 °C. The formazan crystals were then dissolved in DMSO, and the absorbance of each well was measured using a plate reader at a test wavelength of 560 nm. The data are reported as a percentage of cell viability (%) of the treated group compared to untreated cells (control), whose viability is assumed to be 100%.

Cell morphology

To evaluate cell morphology, they were grown in six well/plates and incubated overnight with fresh serum-free DMEM plus 0 (control) and 100 µM solution of the ternary complex. The monolayers were subsequently washed twice with PBS, fixed with methanol and stained with 1:10 dilution of violet crystal for 10 min. Next, they were washed with water and the morphological changes were examined using light microscopy.

ROS, GSH, GSSG and MMP measurements

The production of intracellular reactive oxygen species (ROS) in the A549 cell line was assessed by the oxidation of 2′,7′-dichlorodihydrofluorescein diacetate (H$_2$DCFDA) to 2′,7′-dichloro-fluorescein (DCF), as previously reported.[10] To determine the GSH content, 100 mL aliquots of treated and untreated cells were added to with 1.8 mL of ice-cold phosphate buffer (Na$_2$HPO4 0.1 M-EDTA 0.005 M, pH 8) and 100 mL of o-phthaldialdehyde (OPT) (0.1% in methanol) as described by Hissin and Hilf.[14] To avoid GSH oxidation, the cellular extracts for GSSG measurements were incubated with 0.04 M N-ethyl-maleimide (NEM) before being

mixed with 1.8 mL NaOH 0.1 M and OPT. The fluorescence λ_{em} 420 nm was determined (λ_{ex} 350 nm). The Bradford test was used to determine the protein level of each cellular extract.[15] For the determination of mitochondrial membrane potential (MMP), cells were treated with VONargPhenCl, washed with PBS and stained with 0.4 nM of 3,3′-dihexyloxacarbocyanine iodide, DiOC6 (40 nM stock concentration in DMSO). Changes in MMP ($\Delta\Psi m$) were measured using a Shimadzu RF 6000 fluorometer (excitation/emission = 488 nm/525 nm).[16]

Cellular vanadium uptake experiment

For vanadium uptake experiments, cells were grown to 80% confluence in 100 mm Petri dishes. Incubations with the treatment compounds (100 μM of VONargPhenCl, and VONarg$_2$) were performed for 24 h. Afterwards, V containing media were removed, and the cell layers were washed twice with PBS. Cells were detached using TrypLE enzyme solution for *ca.* 15 min at 37 °C. The cell suspensions were collected into centrifuge tubes and pelleted at 4000 × *g* for 2 min. The cell pellets were washed once with PBS (1.0 mL per tube) and lysed with 100 μL of 0.10 M NaOH overnight at 4 °C. Each lysate (2 μL) was mixed with 98 μL of Bradford reagent and the absorbance at 560 nm was measured using a plate reader for the determination of protein content. Freshly prepared solutions (0–2.0 mg mL^{-1} in 0.10 M NaOH) of bovine serum albumin were used for calibration. The rest of the lysate was diluted to 1.0 mL with 20% HNO$_3$ and vanadium contents were determined using ICP-MS, an accurate and extremely sensitive analytical method that allows quantification of very low levels of intracellular vanadium. Corresponding amounts of NaOH and HNO$_3$ solutions were used to prepare the blank samples. The content of vanadium in the cell lysates was calculated in nmol V per mg protein.[17]

Statistical analysis

Data were analyzed for statistical significance using one-way analysis of variance (ANOVA) followed by Fishers least significant difference (LSD) test and the results were expressed as mean ± SEM.

Results and discussion

Characterization of the solid complex

FTIR spectroscopy. The FTIR spectrum of the complex was compared with the spectra of 1,10-phenanthroline (Phen),[18] naringin and the previously reported binary VONarg$_2$ complex (Fig. S2, ESI†).[7] In the 3400–3200 cm^{-1} region, broad O–H stretching bands were observed, which can be attributed to the presence of R–OH and Ar–OH groups from naringin, as well as OH from the crystallization water. The C=O band of naringin (1645 cm^{-1}) shifted to 1637 cm^{-1} in the VONarg$_2$ complex and to 1612 cm^{-1} in the ternary complex (Table 1). The shift in the C=O vibrational bands suggests that the coordination of this ligand remained similar to that in the binary complex involving the 4-C=O and 5-C–O$^-$ groups. Additionally, the replacement

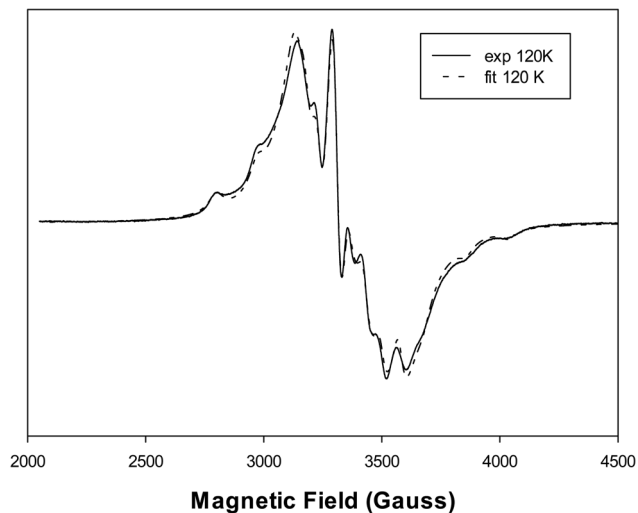**Table 1** Tentative assignments of the FTIR spectra of naringin and the oxidovanadium(IV) complexes (band positions in cm^{-1})[a]

Naringin[7]	VONarg$_2$[7]	VONargPhenCl	Vibrational modes-functional groups
3422 br	3395 br	3389 br	νO–H
3231 sh	3205 sh	3216 sh	
1645 vs	1637 sh	1612 vs	νC=O ring C
1629 sh	1614 vs		νC=C
1615 sh			
1582 m	1574 vs	1579 vs	νC=C
	1537 m	1535 m	
1520 m	1520 m	1520 m	νC=C
1504 m			
1355 sh	1357 sh	1361 w	δCOH
1341 m			
1295 m	1292 w	1291 w	δHOC
1281 w	1256 w	1260 w	δHOC, ν(C–O–C)
1265 w			
1134 s	1134 m	1135 m	νC–O secondary alcohol
1074 vs	1076 vs	1074 vs	νO–C sugar
1062 vs	1060 sh		νC–O primary alcohol
1041 vs	1040 sh	1039 sh	νO–C
987 m	987 m	987 sh	νO–C
	980 m	972 m	νVO
		847 m	Phen
822 m	814 w	814 w	νC–C, νO–C
		724 m	Phen

[a] vs, very strong; s, strong; m, medium w, weak; vw, very weak; br, broad; sh, shoulder.

of one flavonoid ligand by Phen caused a red shift of the C=O stretching band due to π delocalization and a consequent decrease in the bond order of this moiety.[19] The band assigned to the C–O stretching of the sugar moiety (1074 cm^{-1}) remained at the same position in the three compounds, indicating that the glycoside did not interact with the metal center. The most significant changes between the spectra were observed in the VO stretching band and the addition of new bands due to the Phen ligand in the ternary complex. The VO stretching band shifted from 980 cm^{-1} to 972 cm^{-1}, suggesting an increase in bond length and a decrease in bond order after replacing one naringin ligand with Phen. This change might reduce the π electron resonance with the VO cation. In addition, the V=O stretching mode is sensitive to the nature of the *trans*-ligand. Donor ligands in the *trans*-position (anions like chloride, or electron donor ligands, like pyridine) interacted with the empty d-orbital of the metal center and can increase the electron density on the metal ion, producing repulsion of the V=O bond lowering both the V–O multiple bond character and the infrared stretching frequency.[20] Moreover, Phen bands located at 852 cm^{-1} and 738 cm^{-1} assigned to in phase and out of phase ring hydrogen atom motions, shifted to 847 cm^{-1} and 724 cm^{-1} with a decrease in intensity, indicating the coordination of Phen to the metal center.

EPR spectroscopy. The powder EPR spectrum of the complex obtained at room temperature (not shown) exhibited no noticeable differences compared to the spectrum obtained at 120 K (Fig. 2). The EPR spectrum of the powder of VONargPhenCl indicated that the hyperfine splitting with the ^{51}V nucleus (I = 7/2) did not collapse. This finding suggests the absence

Fig. 2 EPR spectra of VONargPhenCl in powder together with simulation. EPR spectrum of the powder was recorded using a Bruker EMX-Plus spectrometer, equipped with a rectangular cavity. Experimental conditions: 100 kHz field modulation field, 4 Gpp modulation amplitude, and 0.6 mW microwave power. The spectrum was baseline corrected using WinEPR Processing software (Bruker, Inc), and simulation was performed with WinEPR Simfonia. The simulation parameters obtained for the powder were $A_{II} = 161 \times 10^{-4}$ cm^{-1}, $g_{II} = 1.946$, $A_{\perp} = 57 \times 10^{-4}$ cm^{-1}, $g_{\perp} = 1.975$.

Fig. 3 Proposed structure of [VONargPhenCl]·$3H_2O$, (VONargPhenCl).

Fig. 4 EPR spectra of VONargPhenCl in frozen DMSO and water/DMSO solutions, together with simulation. EPR spectra were recorded using a Bruker EMX-Plus spectrometer, equipped with a rectangular cavity. Experimental conditions: 100 kHz field modulation field, 4 Gpp modulation amplitude, and 0.6 mW microwave power. The spectra were baseline corrected using WinEPR Processing software (Bruker, Inc), and simulations were performed using EasySpin 5.2.3. toolbox based on MATLAB assuming rhombic and axial spin-Hamiltonians. The simulation parameters obtained for the DMSO solution were $g_{II} = 1.941$, $A_{II} = 165.2 \times 10^{-4}$ cm^{-1}; $g_{\perp} = 1.976$, $A_{\perp} = 59.5 \times 10^{-4}$ cm^{-1}.

of strong spin–spin interactions between neighboring oxidovanadium(IV) ions in the solid complex, which would otherwise lead to a collapse of the hyperfine interaction into a single line, as observed in VOChrysPhenCl and other V$^{(IV)}$ compounds.[21] The simulation parameters ($A_{II} = 161 \times 10^{-4}$ cm^{-1}, $g_{II} = 1.946$, $A_{\perp} = 57 \times 10^{-4}$ cm^{-1}, $g_{\perp} = 1.975$) are consistent with the oxidovanadium(IV) ion being in a pseudoaxial ligand field, and this fits well with a 2N,2O coordination sphere as deduced from the corresponding g_{II} vs. A_{II} diagram.[22]

Considering the elemental analysis determinations, thermogravimetric measurements and FTIR and EPR spectroscopies, the following structure for the solid complex is proposed (Fig. 3).
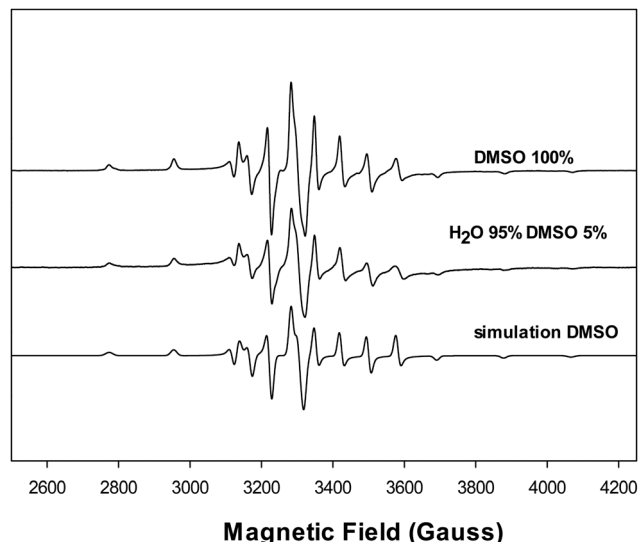
We can discard the formation of a mixture of complexes [VO(Narg)$_2$] and [VO(Phen)$_2$Cl]$^+$ at the pH value of the preparative (pH = 6). The solid complex [VO(Narg)$_2$] was formed at a higher pH value, pH = 9.[7] From speciation measurements, at pH = 6, the speciation for the VO/phen system shows the formation of [VO(Phen)$_2$(OH)]$^+$ as the major species.[23] The species [VO(Phen)$_2$(H$_2$O)]$^{2+}$ is formed at pH = 4.

Characterization of the complex in solution

EPR spectroscopy. The EPR spectra of both the pure DMSO and a water/DMSO 95/5% frozen solutions, measured at 120 K, exhibited similarities and displayed the typical spectrum for axial-V(IV) systems, Fig. 4. The simulation parameters indicated that the oxidovanadium(IV) ion was in a nearly axial or pseudoaxial ligand field. The spin Hamiltonian parameters and the hyperfine coupling constants ($g_{II} = 1.941$, $A_{II} = 165.2 \times 10^{-4}$ cm^{-1}; $g_{\perp} = 1.976$, $A_{\perp} = 59.5 \times 10^{-4}$ cm^{-1}) were found to be very close to those of VOChrysPhen in a DMSO solution

(Chrys, chrysin): $g_{II} = 1.941$; $A_{II} = 162.2 \times 10^{-4}$ cm^{-1}; $g_{\perp} = 1.976$; $A_{\perp} = 59.5 \times 10^{-4}$ cm^{-1}.[19] By considering the empirical relationship between the parallel component of the hyperfine coupling constant (A_z) and the number of equatorial ligands (n_i) and their individual contributions to A_z ($A_{z,i}$), $A_z = \sum n_i A_{z,i}$, the identity of the equatorial ligands around the V(IV) center could be determined.[20] A value for A_{II} of 164.1×10^{-4} cm^{-1} was calculated, in agreement with the experimental A_{II} value, based on the contributions from the following groups: 44.7×10^{-4} cm^{-1} from CO, 38.6×10^{-4} cm^{-1} from ArO^{-}[24] and $2 \times 40.4 \times 10^{-4}$ cm^{-1} from N(Phen) × 2.[25] The results indicate that the binding atoms in the equatorial plane were 2O,2N and the

chloride ion was located in the axial position, *trans*-to the O atom of the oxidovanadium(IV) cation, similar to its arrangement in the solid complex. This suggests a tetragonal compression of the octahedron, as determined by the relationships: $g_\parallel < g_\perp < g_e = 2.0023$ and $|A_\parallel| > |A_\perp|$, where the ground state of the vanadium d^1 ion is defined by the dxy orbital.

For the complexes [VO(Narg)$_2$], [VONargPhenH$_2$O]$^+$ and [VO(Phen)$_2$H$_2$O]$^{2+}$ in solution, the experimental EPR spectra showed the following parallel hyperfine values: $A_{II} = 167.0 \times 10^{-4}$ cm^{-1}, $A_{II} = 165.2 \times 10^{-4}$ cm^{-1} and $A_{II} = 162.7 \times 10^{-4}$ cm^{-1}, for 3 N$_{eq}$, N$_{ax}$, H$_2$O$_{eq}$,[23] respectively. The following values were calculated considering their different environments: VO (4O), VO (2O,2N), VO (3N,O), 166.6×10^{-4} cm^{-1}, 164.1×10^{-4} cm^{-1}, 161.6×10^{-4} cm^{-1},[23] in agreement with the experimental values. It can be seen that the A_{II} values decreased while increasing N-atom coordination. These results demonstrate that the binary species are not seen in the EPR spectra, suggesting that only the ternary complex is formed at pH 6 in the solid phase.

Molar conductivity and electronic spectrum

The molar conductivity values of the complex varied depending on the solvent used. In DMSO, the conductance was found to be 0–14 Ω^{-1} cm^2 mol^{-1} ($t = 0$–24 h), indicating a non-electrolyte nature and no decomposition of the compound during 24 h. A value of 0 Ω^{-1} cm^2 mol^{-1} (DMSO)[7] and 16 Ω^{-1} cm^2 mol^{-1} (95% H$_2$O–5% DMSO) was also obtained for VONarg$_2$, showing that the binary complex behaved as a non-elecrolyte. However, when the VONargPhenCl complex was dissolved in H$_2$O–DMSO (99–1%), the molar conductance increased to 60–80 Ω^{-1} cm^2 mol^{-1} ($t = 0$–24 h). This increase in conductivity can be attributed to the dissociation of the chloride ion, which remains coordinated to the metal center in DMSO but dissociates in water, leading to higher conductivity (Fig. 5).[26,27]

Measurements with intermediate H$_2$O/DMSO ratios showed consistent results: 11–14 Ω^{-1} cm^2 mol^{-1} ($t = 0$–24 h) in 50% DMSO and 50–71 Ω^{-1} cm^2 mol^{-1} ($t = 0$–24 h) in 5% DMSO. The

EPR spectra did not show these effects since the hyperfine parameter is primarily defined by the equatorial plane around the vanadium.

Similarly, the electronic spectrum of the complex in DMSO, Fig. 6, exhibited a d–d electronic transition band at 769 nm ($\varepsilon = 88.4$ M^{-1} cm^{-1}). This band shifted to shorter wavelengths (blue shift) upon the addition of different quantities of water and appeared at 653 nm ($\varepsilon = 130$ M^{-1} cm^{-1}) at 1% DMSO. This shift in the electronic spectrum aligns with the molar conductance measurements. The shift is explained by the replacement of the chloride ligand by the oxygen atom from water, resulting in the formation of the [VONargPhenH$_2$O]$^+$ complex. This change increases the splitting of the d orbitals, causing the electronic transition to occur at higher energy or lower wavenumber, and is an indication that the chloride ion was bonded to the vanadium center.[28] Moreover, the chloride ion in the solution and the cationic complex will generate an increase in the conductivity values.

The stability of the complex was also assessed by measuring the variation of the electronic spectra with time. The results (Fig. S3, ESI†) showed that the complex is stable in DMSO and in 1% DMSO–99% H$_2$O solutions for at least 2 hours. Numerous metallic compounds undergo redox reactions, hydrolysis, and ligand exchange in aqueous media, including biological fluids. These interactions give rise to chemical changes that are influenced by factors such as pH, concentration, and the nature and quantity of various biochemical components. The results of this study, however, allow us to demonstrate that the molecular structure of the complex remains unchanged before its introduction into cell culture.

Antioxidant activity

The antioxidant activity of flavonoids is one of their most important characteristics, and it is responsible for many of their beneficial health effects. As mentioned earlier, the antioxidant activity of flavonoids can be attributed to several
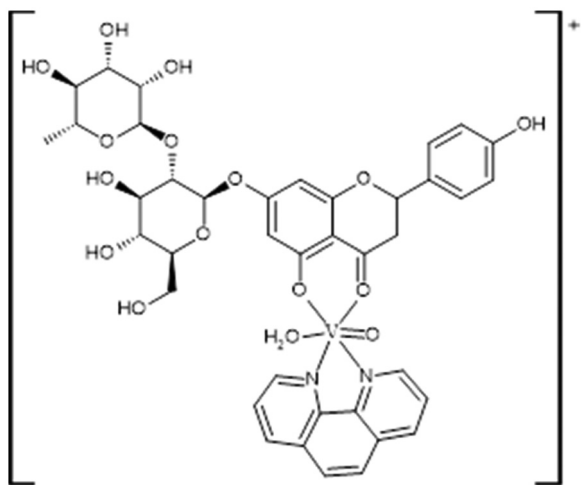

Fig. 5 Proposed structure of [VONargPhenH$_2$O]$^+$ obtained by chloride dissociation of [VONargPhenCl].

Fig. 6 Electronic spectra of VONargPhenCl (2.5×10^{-3} M) in DMSO and mixtures DMSO/H$_2$O (100, 50, 5 and 1% DMSO).

mechanisms: direct scavenging of free radicals, chelation of metal ions, upregulation of enzymatic and non-enzymatic systems involved in the detoxification of oxidizing species, inhibition of enzymes responsible for the production of reactive oxygen species (ROS) and reactive nitrogen species (RNS), regeneration of antioxidant species, such as ascorbate, through electron transfer reactions.

In this study, we evaluated the antioxidant activity of the ternary complex *in vitro* by directly scavenging hydroxyl, superoxide, peroxyl, and 2,2-diphenyl-1-picrylhydrazyl (DPPH$^\bullet$) radicals, Fig. S4 (ESI†). We compared these activities with those of the ligand, the binary complex and the metal ion, previously reported.[7] Table 2 shows the antioxidant effects of the compounds. The ligand Phen did not display superoxide dismutase (SOD) activity and did not scavenge peroxyl, hydroxyl and DPPH radicals.[6]

To determine the capacity of the complex to sequester the $^\bullet$OH radicals, the radicals were generated *in situ* by the ascorbate/Fe/H$_2$O$_2$ system and reacted with deoxyribose which, under acidic conditions, interacted with thiobarbituric acid to give a pink chromogen. Antioxidant agents inhibit the degradation of deoxyribose because they compete with it for the $^\bullet$OH radical, causing a decrease in absorbance at 535 nm. The blank for the spectrophotometric determination was made with the reaction mixture without thiobarbituric acid, considering that the complex exhibited a band with an appreciable intensity at the working wavelength. Sequestering activity was observed at low complex concentrations (15% at 5 μM), a trend that was maintained from 25 μM up to the maximum working concentration of 100 μM, where sequestering activity reached 30%.

The enzyme copper and zinc-dependent superoxide dismutase (Cu, ZnSOD) is a metalloprotein that catalyzes the dismutation of the superoxide anion O$_2^{\bullet-}$. Measuring the activity of the complex to carry out the dismutation of the superoxide radical (similar SOD) consists in generating the radical through the phenazine-methosulfate (PMS)/reduced nicotinamide adenine dinucleotide (NADH) system. These radicals are capable of reducing nitroblue tetrazolium (NBT) to formazan blue that was measured spectrophotometrically. The concentration of the complex that produces 50% inhibition of the reduction of NBT *versus* −log of the concentration of the complex is considered for the determination of the IC$_{50}$ value. While the measured IC$_{50}$ value for the native enzyme is 0.27 μM, a 35.5 μM value determined for the complex is considered as a moderate antioxidant compound against superoxide anion.

The thermal decomposition of AAPH (2,2-azobis(2-amidinopropane)dihydrochloride) generates peroxyl radicals. The lag phase, which signifies the delay of the consumption of pyranine upon the addition of the complex, was determined as the time interval during which peroxyl radicals were consumed before pyranine consumption commenced. This lag phase was measured to evaluate a compound's capability to scavenge ROO$^\bullet$ radicals. The scavenging activity of the ligand and VONarg$_2$ on peroxyl radical was enhanced upon the inclusion of Phen. The ternary complex caused a delay in pyranine consumption (lag phase) by the ROO$^\bullet$ radical of 6.0 min at a concentration of 100 μM.

However, this delay was found to be shorter than the lag phase generated using Trolox (used as reference compound, 37.28 min).

The DPPH$^\bullet$ (2,2-diphenyl-1-picrylhydrazyl) radical is a stable radical with an intense violet color widely used to measure the capacity of direct radical scavenging using an antioxidant compound. To evaluate the antioxidant capacity of the complex against the DPPH$^\bullet$ radical, the absorbance at 517 nm of the solutions with the radical and increasing amounts of the complex was measured by electronic spectroscopy. The DPPH$^\bullet$ anti-radical activity begins at 25 μM complex concentration and grows up to 100 μM (25% activity).

It was observed that complexation of VONarg$_2$ with phenanthroline improved, with respect to the binary complex and the free ligand, the SOD-like activity, and peroxyl and hydroxyl radical scavenging activity. That is, it improved the antioxidant activity against ROS, with respect to the binary complex. The DPPH$^\bullet$ anti-radical activity was improved with respect to the free ligand, but not against the binary complex.

As reported, the ligand naringin is a moderate antioxidant agent, because of the absence of the double bond between the C2–C3 atoms, which does not allow electronic resonance when the flavonoid is transformed into a radical.[7] The improvements in the antioxidant activities by complexation may be due to the coordination of both the flavonoid (involving the C=O and O– groups) and the aromatic ligand phenanthroline with the VO^{2+} cation. The increase in the delocalization of the unpaired electron (which is generated when the flavonoid acts as a radical scavenging agent) by π conjugation, both with the π bond in VO^{2+} and with phenanthroline, produces a more stable radical, generating a greater antioxidant compound, with even greater capacity than the binary complex.

In vitro cellular measurements

Cell viability. The results of cytotoxicity assessments for VONargPhenCl and Phen.Cl conducted using the MTT technique

Table 2 Percentage of free radical scavenging of naringin, VONarg$_2$, oxidovanadium(IV) cation and VONargPhenCl. Values are expressed as the mean ± standard error of at least three independent experiments

		SOD (IC$_{50}$, μM)	ROO$^\bullet$, lag (min), 100 μM	$^\bullet$OH, 100 μM	DPPH$^\bullet$, 100 μM
% Scavenging	Naringin[7]	>1000	0	28.0 ± 0.4	2.0 ± 0.7
	VONarg$_2$[7]	870 ± 5.2	3.8 ± 0.8	0	45.0 ± 5.0
	V(IV)O^{2+}[7]	15.0 ± 0.2	6.4 ± 1.1	38.0 ± 2.0	37.0 ± 2.0
	VONargPhenCl	35.5 ± 3.6	6.0 ± 0.4	29.0 ± 3.0	24.0 ± 1.5

IC$_{50}$ SODnative = 0.21 μM; lag phase Trolox, 37.28 min.

against the A549 cell line after 24 h of exposure, are illustrated in Fig. 7A. The calculated IC_{50} values are presented in Table 3 and are compared with those previously reported for the oxido-vanadium(IV) cation,[29] naringin and $VONarg_2$.[7] The ternary complex demonstrated significantly higher activity compared to the binary complex, with IC_{50} values of 48.44 and >100 M, respectively. This behavior indicates that the replacement of one ligand Narg with a rigid, hydrophobic and planar, N,N-heterocyclic ligand in the complex contributes to enhancing its cytotoxic potential, increasing the lipophilicity and improving cell absorption. This hypothesis is supported by the cell uptake assays (see below). Similar results were observed for the ternary complex with the flavonoid chrysin.[21] It is noteworthy to notice that the cytotoxic activity of the ternary complex after 24 hours of incubation is higher than that of the free ligands, suggesting that the vanadium ion may facilitate cellular penetration of active species.

Furthermore, when evaluating the human amnion WISH cell line, it was not possible to estimate the IC_{50} value for VONargPhenCl, because cell viability was only tested up to 100 μM. The compound moderately reduced the viability of normal cells (by approximately 25% above 5 μM, Fig. 7B). Due to these observations, a selectivity index cannot be established; however, the data indicate that the complex exhibits selectivity for lung cancer cells.
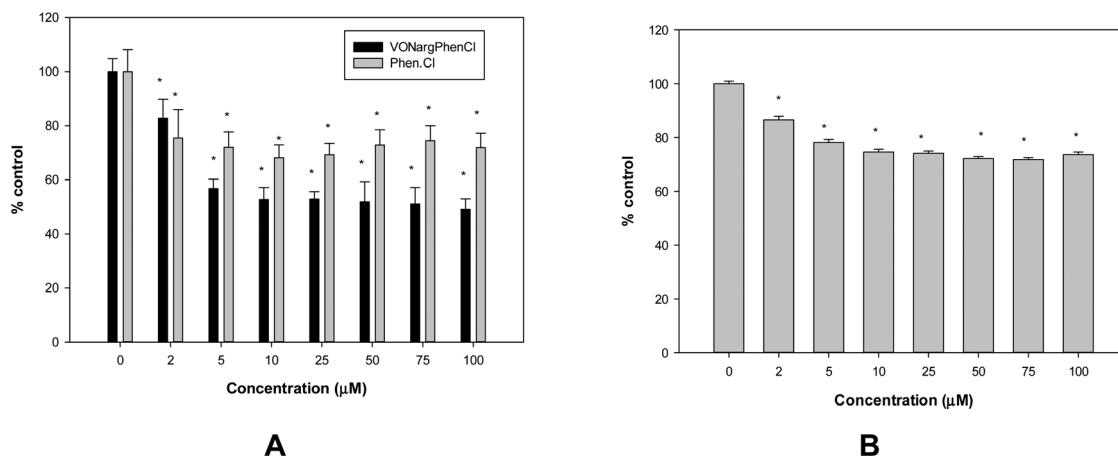
Morphological changes. Untreated A459 cells have a defined epithelial morphology and cell–cell close adhesion[30] whereas 100 μM of VONargPhenCl treatment resulted in a significant increase in the percentage of nuclear-shrinking round cells and a significant reduction in cell number, as seen in Fig. 8. These morphological features are typical of apoptotic cells. Therefore, our findings imply that cell death may be caused by an apoptotic process.

Cellular vanadium uptake. Cellular uptake plays a major role in drug bioactivity. The internalization and accumulation of metal-based drugs within cancer cells are crucial for the effectiveness of tumor therapy. Therefore, the cellular vanadium

Table 3   The results of cytotoxicity testing (expressed as mean IC_{50} values ± S.E.M. calculated out of at least three independent experiments in μM) of VONargPhenCl on the human lung cancer cell line (A549). The cytotoxicity of the complex is compared to the free ligand naringin, the metal V(IV)O^{2+}, the coligand Phen.Cl, and the binary complex $VONarg_2$

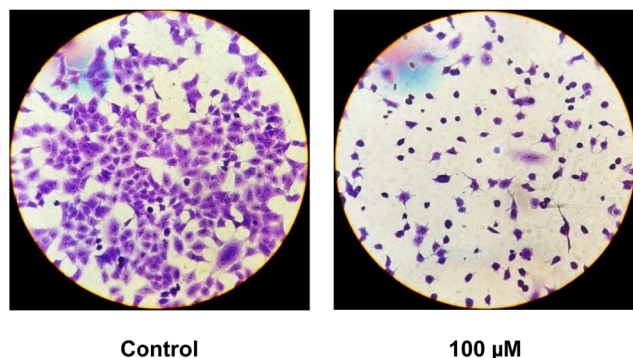|	IC_{50} (μM), 24 h
V(IV)O^{2+} [23]	>100
Naringin[7]	>100
Phen.Cl	>100
$VONarg_2$[7]	>100
VONargPhenCl	48.44 ± 3.91

content was assessed in A549 cells treated with $VONarg_2$ and VONargPhenCl for 24 h to investigate a potential link between their cytotoxic effects and cellular accumulation. Cellular vanadium levels were quantified using inductively coupled plasma-mass-spectrometry (ICP-MS), and the results, expressed as nmol vanadium per mg protein, are presented in Table 4. When compared to the untreated control, the binary complex, at 100 μM, resulted in approximately a 7-fold increase in intracellular vanadium levels, while the ternary complex led to an approximately 11-fold increase at the same concentration. These results can be expressed as a percentage of the administered dose, indicating an uptake of 11.7% for the binary complex and 17.6% for the ternary compound. The VONargPhenCl complex contains a lipophilic ligand in its structure, which may play a crucial role in facilitating its diffusion through the cell membrane and subsequent accumulation within the cell. This information corresponds to the observed trend of IC_{50} values, highlighting how cytotoxic effects are often, at least partially, influenced by cell internalization. Similar results were obtained by Rivas Garcia et al., where the exposure to (bis(maltolato)-oxidovanadium(IV)) of HepG2 cell line increased the cellular content of V in about 8-fold with respect to the untreated cells[31] and for the VOChrysPhen complex[21] with an increase of 5-fold respect to the binary VOchrys complex. On the other hand, Levina et al. demonstrated that intracellular V levels (added as a

Fig. 7 Viability of Phen.Cl and VONargPhenCl on A549 cell line (A) and of VONargPhenCl on WISH cell line (B). The cells were exposed to various doses of the compounds for 24 h. The results are expressed as a percentage of the control level and represent the mean and standard error of the mean (S.E.M.) from three separate trials. * Denotes significant values in compared to the control level ($p < 0.05$).

Fig. 8 Effect of the treatment of A549 cell line with VONargPhenCl on cell morphology. Cells were incubated for 24 h without (control) and with VONargPhenCl (100 μM). Morphology was visualized and photographed under an inverted microscope (magnification, ×250).

Table 4 Cellular V content (determined by ICP-MS) following cell treatments with 100 μM of compounds for 24 h. Results are expressed as mean ± the standard error of the mean (S.E.M.) of two independent experiments
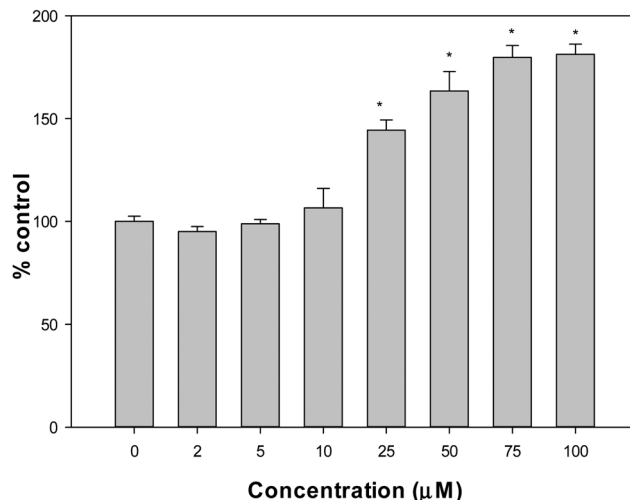
	nmol V mg per protein
Control	1.71 ± 0.50
VONarg$_2$[a]	11.32 ± 0.75
VONargPhenCl[a]	18.45 ± 1.21

[a] This work.

Fig. 9 Effects of VONargPhenCl on ROS production. A549 cells were incubated for 4 h at 37 °C in the presence of 10 μM H$_2$DCFDA which oxidizes to DCF. The values are expressed as a percentage of the control level and represent the mean ± S.E.M. * Indicates significant values in comparison with the control level ($p < 0.05$).

ternary V(v) complex) ranged from 2 to 22 nmol mg^{-1} protein in different cancer cell lines.[17] In A549 cells, the uptake of the metal center, measured as a 10 μM VOSO$_4$·5H$_2$O solution after 72 hours of incubation, exhibited a lower uptake (0.3 nmol V per mg protein).[32] Furthermore, the vanadium uptake of a 28.9 μM solution of [VO(acac)$_2$] (A549 cell line, 24 h incubation) resulted similar to untreated cells value.[21]

Intracellular reactive oxygen species (ROS) generation. In contrast to cancer cells, normal cells exhibit a different redox status that is essentially characterized by a lower rate of ROS production and, consequently, a lower requirement for ROS-scavenging mechanisms.[33] This distinct redox environment in cancer cells can potentially render them more susceptible to therapies that manipulate ROS levels. In this context, the impact of VONargPhenCl treatment on ROS levels was examined using the DCFH-DA staining technique. It was observed that the fluorescence levels for the complex decreased compared to the control levels after 24 h of incubation (data not shown). Given the high rate of cell death, this finding suggests that the probe cannot be retained within the cell. However, after 4 h of incubation, the ternary complex induced a dose-dependent increase in ROS levels (approximately 180% of the control level at 100 μM), as depicted in Fig. 9. In contrast, naringin[7] and oxidovanadium(IV) cation[34] did not significantly elevate ROS levels, while both VONar$_2$[7] and Phen[6] induced increments in ROS levels at 24 h incubation. The results are in line with the observations regarding cell viability.

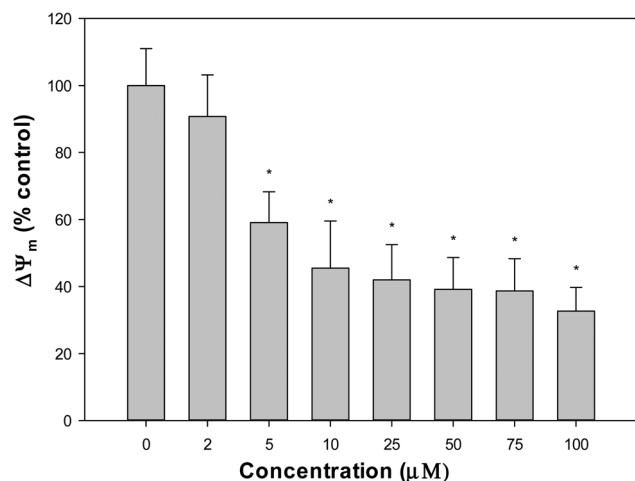**Mitochondrial membrane potential evaluation.** Changes in mitochondrial membrane potential (MMP) are a valuable indicator of mitochondrial function, which is a critical marker of cellular health. In particular, a loss of mitochondrial membrane potential occurs commonly when appropriate drugs induce cancer cell death. To assess the impact of the compound on mitochondria, A549 cells were treated with various doses of VONargPhenCl for 24 h and then exposed to a lipophilic cationic probe, DIOC6, which can penetrate mitochondria. As depicted in Fig. 10, MMP decreased in response to increasing doses of the ternary complex, indicating mitochondrial depolarization, since the probe cannot be accumulated within the organelle.[35]

GSH/GSSG cellular levels. The presence of glutathione (GSH) within the cell is critical because it serves as a non-enzymatic antioxidant defense mechanism. GSH can be oxidized to its disulfide form, GSSG, by various substances, including reactive oxygen species (ROS). In comparison to normal cells, cancer cells often maintain higher intracellular levels of GSH, possibly in response to their elevated metabolism and consequently higher steady-state levels of ROS.[36] Both the levels of GSSG and the changes in the GSH/GSSG ratio are indicative of alterations in the cellular redox balance. In this regard, Fig. 11 shows that increasing concentrations of VONargPhenCl induced a decrease in intracellular GSH levels and the GSH/GSSG ratio. These results suggest that the mechanism of action of VONargPhenCl involves the mitochondrial pathway mediated by an increase in intracellular ROS.

Interaction with bovine serum albumin (BSA). The interaction between biomacromolecules, especially the interaction between plasma proteins and drugs, has been an interesting research field in life sciences, chemistry, and clinical medicine. Bovine serum albumin (BSA) serves as a prototypical protein for drug delivery due to its medical significance, abundance, affordability, ease of purification, ligand binding characteristics, and widespread acceptance in the pharmaceutical

Fig. 10 Changes of the mitochondrial membrane potential (% $\Delta\psi$m) in A549 cells treated with increasing concentrations of VONargPhenCl for 24 h. Each point represents the mean $\pm$ (S.E.M.) of three measurements in three independent experiments. * Indicates significant values in comparison with the control level ($p < 0.05$).

industry. It is widely acknowledged that bovine serum albumin contains two tryptophan residues displaying inherent fluorescence, located at positions 134 and 212, respectively.[37,38]

Upon interaction with the ternary complex, BSA exhibited a reduction in fluorescence intensity (quenching) within the emission spectrum. The mechanism of this interaction can be studied by applying the Stern–Volmer equation to fluorescence data recorded at different temperatures: $F_0/F = 1 + K_{SV}[Q]$ (not shown), where F_0 and F represent the fluorescence intensities in the absence and presence of the quencher, $[Q]$ is the concentration of the quencher, and K_{SV} denotes the Stern–Volmer quenching constant.[39]

The quenching effect can be categorized as static or dynamic. Dynamic quenching is characterized by the increase in K_{SV} with increasing temperature, while static quenching involves a reduction of K_{SV} at higher temperatures.[40] From Table 5, it is evident that the interaction of the complex with BSA is static, resulting in the formation of a complex between the protein and the ternary metal complex.

The number of binding sites on the protein and the binding constant can be determined by plotting the logarithm of $(F_0 - F)/F$ against the logarithm of Q, and applying the subsequent equation: $\log[(F_0 - F)/F] = \log K_b + n \log(Q)$, where K_b denotes the binding constant (y-intercept) and n is the number of binding sites (slope of the line), Fig. S5 (ESI†). The calculated K_b and K_{SV} values are presented in Table 5. The value of n, indicating binding sites, is nearly 1, being in concordance with the presence of almost one binding site for both the ligand and the complex. Furthermore, the binding constants decreased with increasing temperature, with K_b values ranging between 10^4–10^5 M^{-1} range. These K_b values are adequately high to facilitate the complex's transportation by the protein, yet not excessively high to hinder its release at the target site. These results suggest that the complex likely possesses favorable bioavailability, promoting solubility and influencing its distribution at the cellular level both *in vivo* and *in vitro*.[41]

Likewise, the binding mechanism between proteins and small molecules like drugs involves different interaction types associated with thermodynamic parameters, such as hydrophobic forces ($\Delta H > 0$ and $\Delta S > 0$), electrostatic interactions ($\Delta H < 0$ and $\Delta S > 0$), and hydrogen bonding and van der Waals interactions ($\Delta H < 0$ and $\Delta S < 0$). The enthalpy change (ΔH) and entropy change (ΔS) values can be computed from fluorescence measurements at various temperatures using the following equation: $\ln K_b = -\Delta H/RT + \Delta S/R$, where K_b represents the binding constant at different temperatures, R is the universal gas constant (8.31 J mol^{-1} K^{-1}) and T is the temperature in Kelvin. van't Hoff plots ($\ln K_b$ and $1/T$) were used to estimate the ΔH and ΔS values. The free energy change (ΔG) was evaluated in accordance with the thermodynamic relationship: $\Delta G = -RT \ln K_b$. The negative ΔG values obtained at three different temperatures indicate the spontaneous binding of

A

B

Fig. 11 Effect of VONargPhenCl on GSH cellular levels (A) and GSH/GSSG ratio (B) in A549 cells, 24 h incubation. Results are expressed as mean $\pm$ SEM of three independent experiments. * Significant values in comparison with the basal level ($p < 0.05$).

Table 5 Fluorescence experiments. Stern–Volmer constant (K_{SV}), binding constant (K_b) and n binding sites and thermodynamic parameters for the interaction of BSA with VONargPhenCl

T (K)	K_b (M^{-1}) $\times 10^4$	n	K_{SV} (M^{-1}) $\times 10^4$	ΔH° (KJ mol^{-1})	ΔG° (KJ mol^{-1})	ΔS° (KJ mol^{-1} K^{-1})
298	33.85 ± 1.55	1.27 ± 0.04	2.77 ± 0.04	−121.91 ± 6.01	−31.42 ± 1.38	−0.30 ± 0.02
303	13.06 ± 0.76	1.17 ± 0.05	2.51 ± 0.06		−29.90 ± 1.21	
310	4.97 ± 0.27	1.08 ± 0.02	2.49 ± 0.04		−27.83 ± 1.15	

the complex to BSA (Table 5). The calculated negative entropy and enthalpy values imply that the interaction with BSA mainly occurs through the formation of hydrogen bonds and van der Waals interactions.[42]

Comparatively, the binary complex showed higher K_b values than naringin, and these values increased with temperature.[7] The replacement of one naringin ligand with Phen in the ternary complex, led to increased binding at 298 K. However, the strength of the BSA-complex bond is weakened with temperature, resulting in a reduction in the binding constant. Moreover, while naringin and VONarg$_2$ displayed hydrophobic interactions with BSA (indicated by positive ΔH and ΔS values), the ternary complex showed hydrogen bonding and van der Waals interactions. As evidenced by electronic spectroscopy and conductance measurements, the ternary complex substituted the chloride ligand with water, forming the cationic [VONargPhenH$_2$O]$^+$ complex. The distinctive behavior of BSA binding could potentially be attributed to the cationic nature of the new complex in an aqueous environment. Moreover, the different interaction with BSA could be due to the high polarizability of the ligand phen because of the π electronic charge distribution. When the polarizability of the π electron density of the compounds interacting with BSA increases the negative self-association parameters for ΔH and ΔS also increase.[36] Notwithstanding, it can be assumed that this complex could exhibit stability in biological systems and could be transported by albumin.

Conclusions

Flavonoids can interact with metal ions at different metal chelation sites. Metal flavonoid complexes were shown to increase the therapeutic effects of the parent natural phytochemical compounds. In this study, the replacement of one naringin ligand with phenanthroline in the binary complex VO(Narg)$_2$ was achieved, by the synthesis of the VONargPhenCl complex. The solid compound retained the same structure in DMSO solution. However, a ligand substitution reaction (replacement of chloride with water) was suggested when the complex was dissolved in DMSO and increasing amounts of water were added. In any case, both compounds showed stability during the time of manipulation of the solutions, before the addition to the cell culture. The replacement of one ligand by phen, a conjugated system containing delocalized π-electron clouds, provides substantial effects in the free radical scavenging activities. From the experimental data, it is clear that the coordination of the oxidovanadium(IV) complex and the lipophilic ancillary phen ligand had beneficial effects

by increasing cytotoxicity, in the human lung cancer A549 cell line, through the apoptotic pathway. Loss of mitochondrial potential and morphological changes agree with these observations. A pro-oxidant effect was observed for the VONargPhenCl complex, with increased ROS production and GSH/GSSG depletion in correlation with the anti-tumorigenic actions. Moreover, the complex showed selectivity toward tumor cells over non-tumor cells. The introduction of phen increased the lipophilicity of the complex, which could improve cellular uptake and showed favorable binding with BSA.

Author contributions

Conflicts of interest

The authors declare no conflicts of interest.

Acknowledgements

References

1 A. Sharma, P. Bhardwaj and S. Kumar Arya, Naringin: A potential natural product in the field of biomedical applications, *Carbohydr. Polym. Technol. Appl.*, 2021, **2**, 100068, DOI: **10.1016/j.carpta.2021.100068**. ISSN 2666-8939.

2 V. Gelen, S. Yıldırım, E. Sengül, A. Çınar, F. Çelebi, M. Küçükkalem and M. Gök, Naringin attenuates oxidative stress, inflammation, apoptosis, and oxidative DNA damage in acrylamide-induced nephrotoxicity in rats, *Asian Pac. J. Trop. Biomed.*, 2022, **12**, 223, DOI: **10.4103/2221-1691. 343390**.

3 J. A. Adetunji, K. D. Fasae, A. I. Awe, O. K. Paimo, A. M. Adegoke, J. K. Akintunde and M. P. Sekhoacha, The protective roles of citrus flavonoids, naringenin, and naringin on endothelial cell dysfunction in diseases, *Heliyon*, 2023, **9**, e17166, DOI: **10.1016/j.heliyon.2023.e17166**.

4 A. M. Mahmoud, F. L. Wilkinson, M. A. Sandhu, J. M. Dos Santos and M. Y. Alexander, Modulating Oxidative Stress in Drug-Induced Injury and Metabolic Disorders: The Role of Natural and Synthetic Antioxidants, *Oxid. Med. Cell. Longevity*, 2019, 3206401, DOI: **10.1155/2019/3206401**.

5 R. R. Crichton, *Biological Inorganic Chemistry: A New Introduction to Molecular Structure and Function*, Elsevier, Academic Press, 3rd edn, 2019. ISBN: 978-0-12-811741-5.

6 L. G. Naso, J. J. Martínez Medina, F. D'Alessandro, M. Rey, A. Rizzi, O. E. Piro, G. A. Echeverría, E. G. Ferrer and P. A. M. Williams, Ternary copper(ɪɪ) complex of 5-hydroxytryptophan and 1,10-phenanthroline with several pharmacological properties and an adequate safety profile, *J. Inorg. Biochem.*, 2020, **204**, 110933, DOI: **10.1016/j.jinorgbio.2019.110933**. ISSN 0162-0134.

7 A. G. Restrepo-Guerrero, H. Goitia-Semenco, L. G. Naso, M. Rey, P. J. Gonzalez, E. G. Ferrer and P. A. M. Williams, Antioxidant and Anticancer Activities and Protein Interaction of the Oxidovanadium(ɪᴠ) Naringin Complex, *Inorganics*, 2022, **10**, 13, DOI: **10.3390/inorganics10010013**.

8 L. Naso, E. G. Ferrer and P. A. M. Williams, Correlation of the anticancer and pro-oxidant behavior and the structure of flavonoid-oxidovanadium(ɪᴠ) complexes, *Coord. Chem. Rev.*, 2023, **492**, 215271, DOI: **10.1016/j.ccr.2023.215271**.

9 H. Onishi, *Photometric determination of traces of metals*, John Wiley and Sons, Inc, New York, 4th edn, 1986.

10 J. J. Martínez Medina, L. G. Naso, A. L. Pérez, A. Rizzi, N. B. Okulik, E. G. Ferrer and P. A. M. Williams, Apigenin oxidovanadium(ɪᴠ) cation interactions. Synthesis, spectral, bovine serum albumin binding, antioxidant and anticancer studies, *J. Photochem. Photobiol., A*, 2017, **344**, 84–100, DOI: **10.1016/j.jphotochem.2017.05.007**.

11 E. P. Kirby in *Excited States of Proteins and Nucleic Acids*, ed. R. F. Steiner and I. Weinryb, Springer US, Boston, MA, 1971, DOI: **10.1007/978-1-4684-1878-1**.

12 S. H. Peng, B. B. Lv, A. Ali, J. M. Wang, X. Ying, H. Wang, J. B. Liu, L. N. Ji and H. Y. Liu, The Magnetic Properties, DNA/HSA Binding and Nuclease Activity of Manganese N-Confused Porphyrin, *J. Porphyrins Phthalocyanines*, 2016, **20**, 624–638, DOI: **10.1142/S1088424616500449**.

13 L. Hayflick, The establishment of a line (WISH) of human amnion cells in continuous cultivation, *Exp. Cell Res.*, 1961, **3**, 14–20, DOI: **10.1016/0014-4827(61)90059-3**.

14 P. J. Hissin and R. Hilf, A fluorometric method for determination of oxidized and reduced glutathione in tissues, *Anal. Biochem.*, 1976, **74**, 214–226, DOI: **10.1016/0003-2697(76)90326-2**.

15 M. M. Bradford, A rapid and sensitive method for the quantitation of microgram quantities of protein utilizing the principle of protein-dye binding, *Anal. Biochem.*, 1976, **72**, 248–254, DOI: **10.1016/0003-2697(76)90527-3**.

16 Y. Akkoç, O. Berrak, E. Arısan, P. Obakan, A. Çoker-Gurkan and N. Palavan-Unsal, Inhibition of PI3K signaling triggered apoptotic potential of curcumin which is hindered by Bcl-2 through activation of autophagy in MCF-7 cells, *Biomed. Pharmacother.*, 2015, **71**, 161–171, DOI: **10.1016/j.biopha.2015.02.029**.

17 A. Levina, A. Pires Vieira, A. Wijetunga, R. Kaur, J. Koehn, D. Crans and P. Lay, A Short-Lived but Highly Cytotoxic Vanadium(ᴠ) Complex as a Potential Drug Lead for Brain Cancer Treatment by Intratumoral Injections, *Angew. Chem., Int. Ed.*, 2020, **59**, 15834–15838, DOI: **10.1002/anie.202005458**.

18 M. S. Islas, J. J. Martínez Medina, O. E. Piro, G. A. Echeverría, E. G. Ferrer and P. A. M. Williams, Comparisons of the spectroscopic and microbiological activities among coumarin-3-carboxylate, *o*-phenanthroline and zinc(ɪɪ) complexes, *Spectrochim. Acta, Part A*, 2018, **198**, 212–221, DOI: **10.1016/j.saa.2018.03.003**.

19 T. Ajaykamal, M. Köckerling and M. Palaniandavar, Copper(ɪɪ)-flavonolate complexes of 2N ligands as functional models for quercetin 2,4-dioxygenase enzymes: The role of axially coordinated water and ligand substitution on dioxygenase activity, *Inorg. Chim. Acta*, 2023, **556**, 121673, DOI: **10.1016/j.ica.2023.121673**.

20 R. A. Nyquist, R. O. Kagel, M. A. Leugers, R. A. Nyquist and C. L. Putzig, *The handbook of infrared and Raman spectra of inorganic compounds and organic salts*, Academic Press, 1997.

21 A. Actis Dato, L. G. Naso, M. Rey, P. J. Gonzalez, E. G. Ferrer and P. A. M. Williams, Phenanthroline Complexation Enhances the Cytotoxic Activity of the VO-Chrysin System, *Inorganics*, 2022, **10**, 4, DOI: **10.3390/inorganics10010004**.

22 N. D. Chasteen, in *Biological Magnetic Resonance*, ed. L. J. Berliner and J. Reuben, Plenum Press, New York, 1981, vol. 3, pp. 53–119.

23 D. Sanna, P. Buglyó, A. I. Tomaz, J. Costa Pessoa, S. Borović, G. Micera and E. Garribba, VIVO and CuII complexation by ligands based on pyridine nitrogen donors, *Dalton Trans.*, 2012, **41**, 12824–12838, DOI: **10.1039/c2dt31109g**.

24 E. G. Ferrer, M. V. Salinas, M. J. Correa, L. Naso, D. A. Barrio, S. B. Etcheverry, L. Lezama, T. Rojo and P. A. M. Williams, Synthesis, characterization, antitumoral and osteogenic activities of Quercetin vanadyl(ɪᴠ) complexes, *J. Biol. Inorg. Chem.*, 2006, **11**, 791–801, DOI: **10.1007/s00775-006-0122-9**.

25 J. Benítez, L. Becco, I. Correia, S. M. Leal, H. Guiset, J. Costa Pessoa, J. Lorenzo, S. Tanco, P. Escobar, V. Moreno, B. Garat and D. Gambino, Vanadium polypyridyl compounds as potential antiparasitic and antitumoral agents: New achievements, *J. Inorg. Biochem.*, 2011, **105**, 303–312, DOI: **10.1016/j.jinorgbio.2010.11.001**.

26 L. F. Chin, S. M. Kong, H. L. Seng, K. S. Khoo, R. Vikneswaran, S. G. Teoh, M. Ahmad, S. B. A. Khoo, M. J. Maah and C. H. Ng, Synthesis, characterization and biological properties of cobalt(ɪɪ) complexes of 1,10-phenanthroline and maltol, *J. Inorg. Biochem.*, 2011, **105**, 339–347, DOI: **10.1016/j.jinorgbio.2010.11.018**.

27 W. J. Geary, The use of conductivity measurements in organic solvents for the characterization of coordination compounds, *Coord. Chem. Rev.*, 1971, **7**, 81–122.

28 F. A. Cotton and G. Wilkinson, *Advanced Inorganic Chemistry*, John Wiley & Sons, New York, 3rd edn, 1972.

29 M. S. Islas, L. G. Naso, L. Lezama, M. Valcarcel, C. Salado, M. Roura-Ferrer, E. G. Ferrer and P. A. M. Williams, Insights into the mechanisms underlying the antitumor activity of an oxidovanadium(ɪv) compound with the antioxidant naringenin. Albumin binding studies, *J. Inorg. Biochem.*, 2015, **149**, 12–24, DOI: **10.1016/j.jinorgbio.2015.04.011**.

30 R. Z. Ren, H. B. Yu, J. S. Li, J. L. Shen and W. S. Du, Suitable parameter choice on quantitative morphology of A549 cell in epithelial-mesenchymal transition, *Biosci. Rep.*, 2015, **35**, e00202, DOI: **10.1042/BSR20150070**.

31 L. Rivas-García, J. L. Quiles, A. Varela-López, M. Arredondo, P. Lopez, A. Rodríguez Diéguez, M. Montes-Bayon, P. Aranda, J. Llopis and C. Sánchez-González, *In vitro* study of the protective effect of manganese against vanadium-mediated nuclear and mitochondrial DNA damage, *Food Chem. Toxicol.*, 2020, **135**, 110900, DOI: **10.1016/j.fct.2019.110900**.

32 A. Levina and P. A. Lay, Vanadium(v/ɪv)–Transferrin Binding Disrupts the Transferrin Cycle and Reduces Vanadium Uptake and Antiproliferative Activity in Human Lung Cancer Cells, *Inorg. Chem.*, 2020, **59**(22), 16143–16153, DOI: **10.1021/acs.inorgchem.0c00926**.

33 A. Glasauer and N. S. Chandel, Targeting antioxidants for cancer therapy, *Biochem. Pharmacol.*, 2014, **92**, 90–101, DOI: **10.1016/j.bcp.2014.07.017**.

34 L. G. Naso, L. Lezama, M. Valcarcel, C. Salado, P. Villacé, D. Kortazar, E. G. Ferrer and P. A. M. Williams, Bovine serum albumin binding, antioxidant and anticancer properties of an oxidovanadium(ɪv) complex with luteolin, *J. Inorg. Biochem.*, 2016, **157**, 80–93, DOI: **10.1016/j.jinorgbio.2016.01.021**.

35 S. W. Perry, J. P. Norman, J. Barbieri, E. B. Brown and H. A. Gelbard, Mitochondrial membrane potential probes and the proton gradient: a practical usage guide, *Biotechniques*, 2011, **50**, 98–115, DOI: **10.2144/000113610**.

36 G. Batist, R. L. Schecter and M. A. Alaoui-Jamali, The glutathione system and drug resistance, in *Principles of antineoplastic drug development and pharmacology*, ed. R. L. Shilsky, G. D. Milano and M. J. Ratain, Dekker, New York, 1996, pp. 503–521. ISBN-10: 0824793145, ISBN-13: 978-0824793142.

37 J. J. Martínez Medina, L. G. Naso, A. L. Pérez, A. Rizzi, E. G. Ferrer and P. A. M. Williams, Antioxidant and Anticancer Effects and Bioavailability Studies of the Flavonoid Baicalin and Its Oxidovanadium(ɪv) Complex, *J. Inorg. Biochem.*, 2017, **166**, 150–161, DOI: **10.1016/j.jinorgbio.2016.11.005**.

38 Y. Moriyama, D. Ohta, K. Hachiya, Y. Mitsui and K. Takeda, Fluorescence Behavior of Tryptophan Residues of Bovine and Human Serum Albumins in Ionic Surfactant Solutions: A Comparative Study of the Two and One Tryptophan(s) of Bovine and Human Albumins, *J. Protein Chem.*, 1996, **15**, 265–272, DOI: **10.1007/BF01887115**.

39 J. R. Lakowicz, *Principles of Fluorescence Spectroscopy*, Springer Science & Business Media, New York, NY, USA, 2013, DOI: **10.1007/978-0-387-46312-4**.

40 L. K. Fraiji, D. M. Hayes and T. C. Werner, Static and dynamic fluorescence quenching experiments for the physical chemistry laboratory, *J. Chem. Educ.*, 1992, **69**, 424–428.

41 Y. Zhang, S. Shi, X. Sun, X. Xiong and M. Peng, The effect of Cu^{2+} on interaction between flavonoids with different C-ring substituents and bovine serum albumin: Structure-affinity relationship aspect, *J. Inorg. Biochem.*, 2011, **105**, 1529–1537, DOI: **10.1016/j.jinorgbio.2011.08.007**.

42 P. D. Ross and S. Subramanian, Thermodynamics of Protein Association Reactions: Forces Contributing to Stability, *Biochemistry*, 1981, **20**, 3096–3102, DOI: **10.1021/bi00514a017**.